

RESEARCH

Open Access



Identification of a novel *FGF3* variant and a new phenotype in three LAMM syndrome families

Qiang Du^{1,2,3†}, Yike Zhang^{1,2†}, Rujian Hong^{4†}, Nuermaimaiti Tulamaiti³, Maiheba Abulaiti³, Nueraili Awuti³, Wulamu Wusiman³, Xirinayi Alimu³, Ayinuer Wusiman³, Nueraihaimaiti Kadier³, Huilin Li³, Zhifei Zhang³, Huan Qi³, Zhipeng Xia⁴, Ayituersun Abudukeyoumu³, Huawei Li^{1,2,5,6,7*} and Luo Guo^{1,2*}

Abstract

Over 700 syndromes associated with hearing loss (HL) have been identified. Labyrinthine aplasia, microtia, and microdontia (LAMM syndrome, OMIM: 610706) is a rare HL syndrome characterized by congenital sensorineural HL, labyrinthine aplasia, type I microtia and microdontia, which is caused by biallelic variants in the *FGF3* gene. Using Whole-exome sequencing (WES), we identified a novel missense *FGF3* variant (c.137G>C, p. Arg46Pro (NM_005247.4)) in three unrelated Uyghur ethnic families. This variant is classified as a variant of uncertain significance according to ACMG guidelines, with the applied criteria of PM3, PM2_Supporting, PP3 and PP4. Patients from the three families revealed variable clinical features. We found a novel phenotype, sparse hair, in one of the proband. Our findings expanded the variant and phenotype spectrum of LAMM syndrome and provided new insights to the diagnose and pathogenesis investigation of the disease.

Keywords Labyrinthine aplasia, Microtia and microdontia, Sensorineural hearing loss, Whole-exome sequencing (WES)

[†]Qiang Du, Yike Zhang and Rujian Hong these authors contributed equally to this work.

*Correspondence:

Huawei Li

hwli@shmu.edu.cn

Luo Guo

guoluo.gary@foxmail.com

¹Department of the Affiliated Eye and ENT Hospital, State Key Laboratory of Medical Neurobiology, ENT Institute and Otorhinolaryngology, Fudan University, Shanghai 200031, China

²NHC Key Laboratory of Hearing Medicine, Fudan University, Shanghai 200031, China

³Department of Otorhinolaryngology, Kashi Prefecture Second People's Hospital, Xinjiang Uygur Autonomous Region, Xinjiang 844000, China

⁴Department of Radiology, Eye & ENT Hospital, Fudan University, Shanghai 200031, China

⁵Institutes of Biomedical Sciences, Fudan University, Shanghai 200032, China

⁶Shanghai Engineering Research Centre of Cochlear Implant, Shanghai 200031, China

⁷The Institutes of Brain Science and the Collaborative Innovation Center for Brain Science, Fudan University, Shanghai 200032, China



Introduction

Hearing loss (HL) is one of the most prevalent sensory disorders that affects 1 to 2 per 1000 children at birth or during childhood [1]. About 60% of congenital HL are caused by genetic factors, 30% are acquired and 10% are idiopathic [2]. Syndromic HL refers to hearing impairment related to abnormalities that affect other organs/systems [3]. Up to now, over 700 syndromes associated with HL have been identified. Nearly 20% of congenital HL is syndromic [3, 4]. HL can be classified as conductive HL, which is related to abnormalities in the external or middle ear and sensorineural HL, which is caused by defects in the inner ear, auditory nerve or auditory cerebral cortex [5]. Structure defects in the inner ear occurs in 15–20% of cases with severe or profound sensorineural HL [6].

Labyrinthine aplasia, microtia, and microdontia (LAMM syndrome, OMIM: 610706) is a rare HL syndrome characterized by congenital sensorineural HL, labyrinthine aplasia, type I microtia and microdontia. It was first described by Tekin et al. in 2007 [7]. Variable features have been described in LAMM patients, including unilateral microtia and normal external ears, hypoplasia of alae nasi and involvement of the middle ear structures. Hearing phenotype of LAMM is typically congenital bilateral profound HL [8]. Although cognitive abilities are normal, patients often reported motor delay, due to absence of vestibular organs. Until now, the prevalence of LAMM syndrome (OMIM 610706, LAMM) has not been established [7].

LAMM is caused by *FGF3* gene in an autosomal recessive manner. *FGF3* gene, also called *Int2* or *HBGF-3*, contains three exons and encodes a 239-amino-acid-long protein, fibroblast growth factor 3 [9]. *FGF3* protein regulates morphogenesis, embryonic development, cell growth, and tumor development through the RAS/MAP kinase pathway [10, 11]. Both loss of function (nonsense, frameshift and splicing) and missense variants affecting highly conserved residues in *FGF3* were found to cause LAMM [12–14]. Furthermore, *Fgf3*-null mouse models showed variable dorsal otic malformations, suggesting that LAMM syndrome is caused by loss of *FGF3* functions [10].

In this study, we recruited three unrelated HL families with LAMM syndrome phenotypes. High throughput sequencing identified a novel missense *FGF3* variant in all three families. Although sharing the same variant, patients from the three families showed variable clinical features.

Materials and methods

Cohort and clinical assessment

Three Uyghur ethnic families were recruited to the Hereditary Deafness Center at the Eye, Otolaryngology

Hospital Affiliated with Fudan University, Shanghai, China. All individuals and family members underwent complete physical examination and were tested by pure-tone audiometry. Hearing thresholds were measured at the following frequencies: 0.125, 0.25, 0.5, 1, 2, 4, 6, and 8 kHz. Patients were examined to identify the inner ear defects by High-resolution magnetic resonance imaging (MRI) scans and High-Resolution CT. Fully informed written consents were provided by all family members. This study was approved by the ethics committee of the Institutional Review Board of the Eye, Ear, Nose and Throat Hospital affiliated with Fudan University (Shanghai, China).

Next-generation sequencing

Whole blood samples were collected, and genomic DNA was extracted using DNA Isolation Kit (Qia-Gen, Hilden, Germany). Proband was pre-screened for pathogenic variants in the *GJB2* gene by Sanger sequencing, and no pathogenic variants were identified. All probands of the families underwent WES subsequently. A sequencing library was prepared using a DNA library preparation kit (New England Biolabs, Ipswich, MA, catalogue#E6040). High-throughput sequencing was performed on Illumina HiSeq 2000 (Illumina, Inc., San Diego, CA). To validate the variant, PCR and sequencing primers were designed by Primer3 online software (<http://bioinfo.ut.ee/primer3/>). PCR and sequencing primers were designed using Primer3 online tools. Sanger sequencing was performed using Primer3 on a 3730XL (Applied Biosystems). The results of Sanger sequencing were aligned and viewed with the reference genome of the *FGF3* gene using the Snapgene tool.

Variant prioritization and interpretation

Raw sequencing data was generated by the Illumina CASAVA v1.8 pipeline and aligned to the human reference genome (hg19) using the Burrows-Wheeler Aligner (BWA) program. Variant calling was done with GATK package v4.1.8.1. All variants were annotated using ANNOVAR software [15]. To identify the pathogenic variants, these variants were filtered out based on the following conditions: (1) low-coverage variants (depth < 10) (2) variants in the noncoding regions (3) synonymous variants in the coding region (4) variants with minor allele frequency (MAF) > 0.001 in several databases (1000 genome project, gnomAD v2.1.1) (5) variants labelled as “benign” in the ClinVar database [15].

In silico analysis of novel candidate variants and gene

The deleterious effect of variants was predicted by Variant Effect Scoring Tool (VEST4), “The Rare Exome Variant Ensemble Learner”(REVEL), (<https://sites.google.com/site/revelgenomics/>), Mendelian Clinically Applicable

Pathogenicity (M-CAP) (<https://bejerano.stanford.edu/mcap/>), mutation tasting (<https://www.mutationtaster.org>), Mutpred2 (<http://mutpred.mutdb.org/index.html>) and AlphaMissense (<https://alphamissense.hegelab.org>). The Ensembl Genome Browser (<http://grch37.ensembl.org/index.html>) and OMIM (Online Mendelian Inheritance in Man) (<http://www.ncbi.nlm.nih.gov/Omim/>) were used to analyze all genes and variants. Variant interpretation was performed based on the American College of Medical Genetics and Genomics (ACMG) recommendations [16, 17]. The ACMG is a report issued for clinically indicated exome and genome sequencing, a minimum list of conditions, genes and variants are supposed to be evaluated and reported to the clinicians [17]. Protein sequences from various species were obtained through NCBI website (<https://www.ncbi.nlm.nih.gov>) and protein sequences from species were aligned using Clustal Omega in SnapGene. The 3D structure of the FGF3 protein was predicted by using the AlphaFold Protein Structure Database (<https://alphafold.ebi.ac.uk>).

Results

Clinical presentation

Case 1

In family 1, the proband was a 6-year-old female with moderate to severe bilateral congenital HL, bilateral microtia and microdontia. She was the third of three children born to nonconsanguineous parents of Uyghur descent. Family history was negative and the pedigree of the family is shown in Fig. 1a. The proband showed bilateral microtia with a shortened upper half of auricles and anteverted ears. Large skin tags at the superior medial aspect of the helical rim were noted bilaterally (Fig. 2a). A long face as well as widely spaced teeth with loss of tooth height and thin enamel (compatible with microdontia) were observed (Fig. 2b and c). Her hair was thin and sparse. Audiogram revealed a moderately severe U-shaped middle-frequency hearing loss (Fig. 2d). MRI scan shows stenosis of the internal auditory canal (Fig. S5a). The results of the MRI illustrate an arachnoid

cyst in cisterna occipitalis magnus, bilateral maxillary sinusitis, enlarged bilateral retropharyngeal lymph nodes.

Case 2

In family 2, the proband was a 10-year-old Uyghur ethnic female with complete labyrinthine aplasia, microtia, and microdontia. She was the first of two children born to consanguineous parents. Her 7-year-old brother was healthy. Family history was negative and the parents were first cousins. The pedigree of the family is shown in Fig. 1b. Bilateral microtia with shortened upper half of auricles and anteverted ears were observed. Large skin tags at the superior medial aspect of the helical rim were noted bilaterally (Fig. 3a). A long face, hypoplastic alae nasi as well as widely spaced teeth with loss of tooth height and thin enamel (compatible with microdontia) were observed (Fig. 3b and c). The audiogram revealed a severe U-shaped middle-frequency hearing loss (Fig. 3d). HRCT show stenosis of the internal auditory canal. Bilateral rudimentary otocysts are evident (Fig. S5b).

Case 3

In family 3, a 1-year-old male and a 12-year-old female were diagnosed with complete labyrinthine aplasia, microtia, and microdontia. Family history was negative and the parents were first cousins. The pedigree of the family is provided in Fig. 1c. The individual's grandmothers are full sisters. The prominent tip of the low set, anteverted, dysplastic left and right ears were observed in the brother and his sister (Fig. 4a and c). Intraoral view shows small widely spaced teeth and abnormal primary canines and molars in the brother and his sister (Fig. 4b and d). Auditory brainstem response (ABR) tests of the proband and her affected brother showed no response at 97dBnHL intensity and the Auditory Steady-State Response (ASSR) tests for air conduction were shown in Fig. 4c. Axial HRCT obtained at the IAC level shows stenosis of the internal auditory canal (Fig. 5).

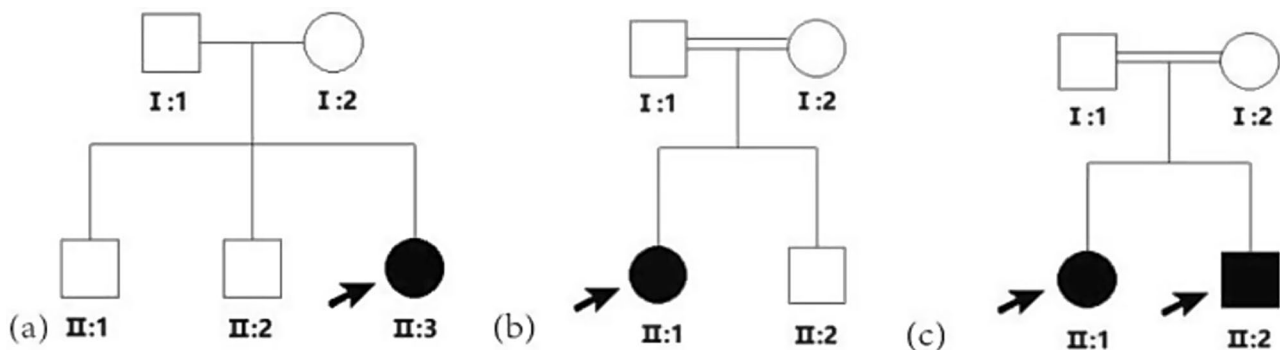


Fig. 1 The pedigrees of the three families. (a). The pedigree of the family (1) (b). The pedigree of the family (2) (c). The pedigree of the family (3) (Arrows indicate the probands)

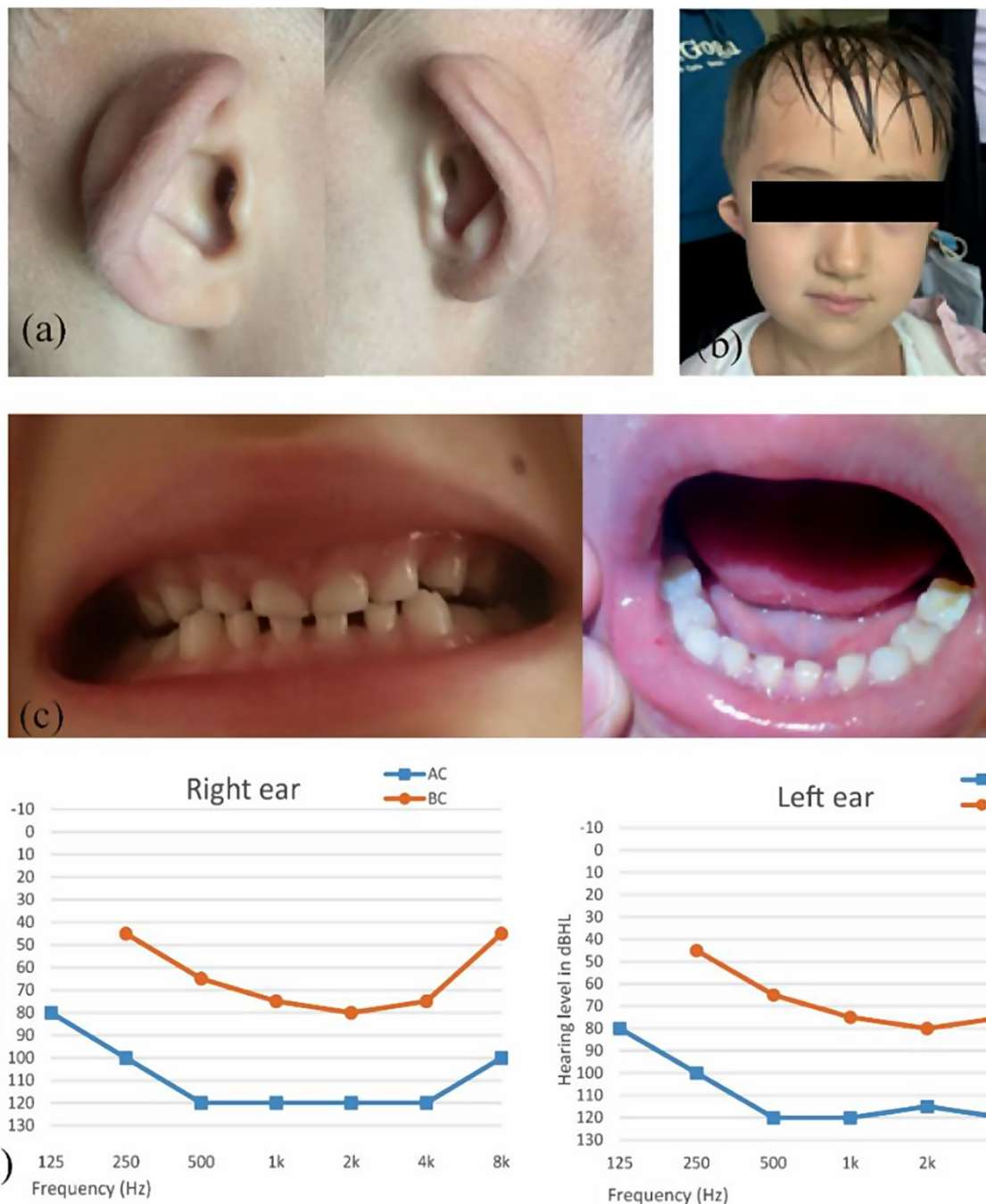


Fig. 2 Clinical photographs of the affected individual in family 1. Note the presence of LAMM syndrome in this patient. (a). The prominent tip of the low set, antverted, dysplastic left and right ears. (b). Sparse hair and a long face were observed. (c). Intraoral views show small widely spaced teeth and abnormal primary canines and molars. (d). Pure-tone audiogram with 125 Hz to 8000 Hz for affected proband (AC means air conduction, BC means bone conduction)

Genetic diagnosis

WES was performed on the probands. A homozygous variant *c.137G>C*, p. Arg46Pro (NM_005247.4), was identified in exon 1 of the *FGF3* gene in all probands of the three families. No pathogenic variants from other known HL genes were identified. This variant was validated by Sanger sequencing in all members of the

family subsequently in three families. The *c.137G>C* variant leads to an amino acid substitution from arginine to proline at codon 46 (p. Arg46Pro) in *FGF3*. Sanger sequencing showed that all four patients were homozygous for this variant, while their parents were all heterozygous (PM3) (Figs. 6, 7 and 8). This variant is predicted to be harmful by multiple prediction tools

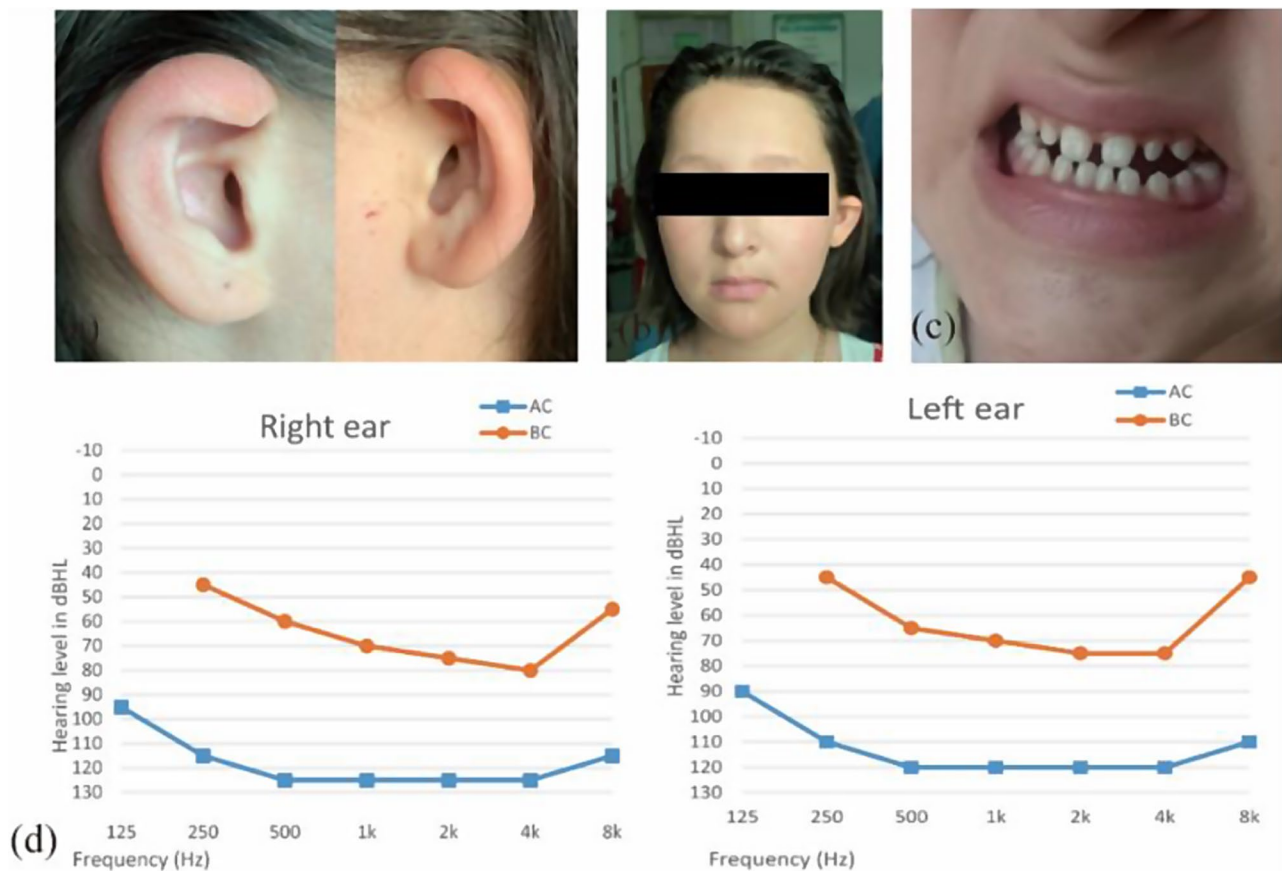


Fig. 3 Clinical photographs of the affected individual in family 2. Note the presence of LAMM syndrome in this patient. (a). The prominent tip of the low set, antverted, dysplastic left and right ears. (b). A long face and hypoplastic alae nasi were observed. (c). Intraoral views show small widely spaced teeth and abnormal primary canines and molars. (d). Pure-tone audiogram with 125 Hz to 8000 Hz for affected proband (AC means air conduction, BC means bone conduction)

(VEST4 score=0.815) (PP3) and prediction results are listed in Table 1. This variant was extremely rare (frequency=0.0000007) in the gnomAD v4.0.0 database (PM2_Supporting). Furthermore, all patients revealed phenotypes highly similar for LAMM syndrome (PP4). Therefore, this variant is classified as a variant of uncertain significance according to ACMG guidelines, with the applied criteria of PM3, PM2_Supporting, PP3 and PP4 [16, 17].

Bioinformatic analysis

The missense variant c.137G>C (p. Arg46Pro) substitutes Arginine with Proline, a nonpolar side chain amino acid, at codon 46 of the FGF3 protein. Arginine is highly conserved at codon 46 of FGF3 among different species (Fig. 9), supporting a pathogenic role for its substitution. Molecular modelling of the mutant protein was performed using Missense3D with AlphFold model AF-P11487-F1. It was suggested that the missense variant replaced a buried charged residue (Arginine) with an uncharged residue (Proline), which might disrupt the H-bonds formed by the original residue. Besides,

the original Arginine has a high pLDDT score (95.96) (Fig. 10).

Discussion

In this study, we recruited three unrelated families with LAMM syndrome. A novel missense variant in exon 1 of the FGF3 gene was identified. Although LAMM syndrome is mainly characterized by HL with labyrinthine aplasia, microtia, and microdontia, other features were also revealed by recent studies, including large skin tags, defect of the middle ear, hypoplastic alae nasi, stenosis of the jugular foramen, and absence or narrowing of the eighth cranial nerve [18]. Although all three families shared the same variant, their clinical manifestations varied. The proband from family 1 showed sparse hair which was not discovered in the other two families or previous LAMM cases. Patient in family 2 revealed hypoplastic alae nasi whereas the other two families were normal. These findings provide further evidence for the variable and diverse features of LAMM syndrome patients.

Until now, more than 24 pathogenic variants in the FGF3 gene have been associated with LAMM syndrome

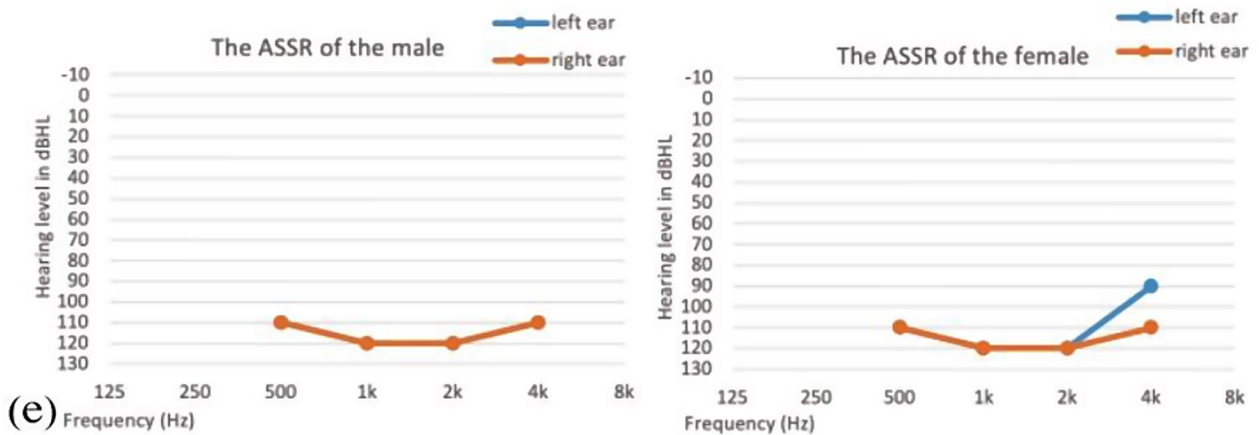
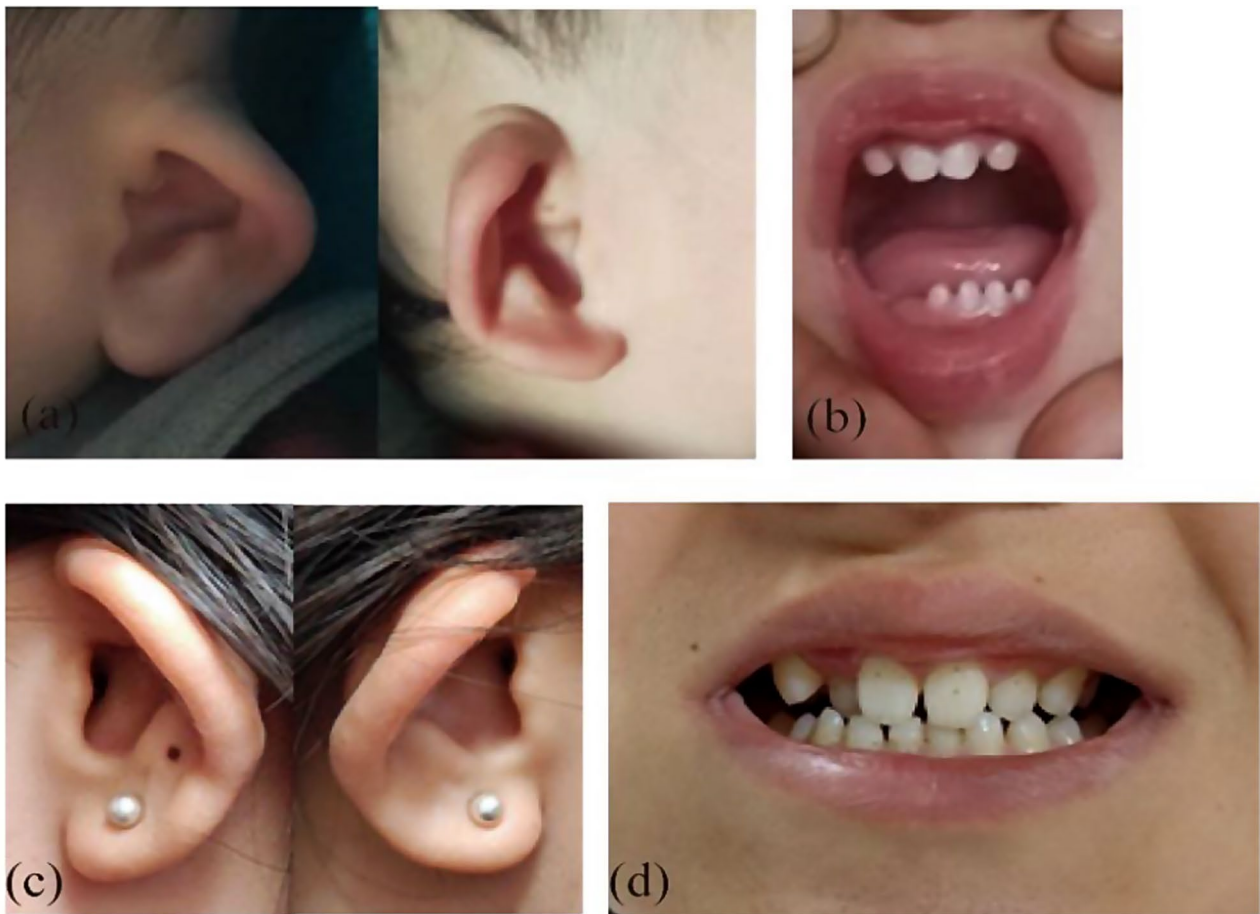


Fig. 4 Clinical photographs of the affected individual in family 3. Note the presence of LAMM syndrome in the patients. **(a, c)**. The prominent tip of the low set, antverted, dysplastic left and right ears of the brother and sister respectively. **(b, d)**. Intraoral views show small widely spaced teeth and abnormal primary canines and molars in the brother and his sister. **(f)**. Auditory Steady-State Response (ASSR) tests for air conduction with 125 Hz to 8000 Hz for affected probands

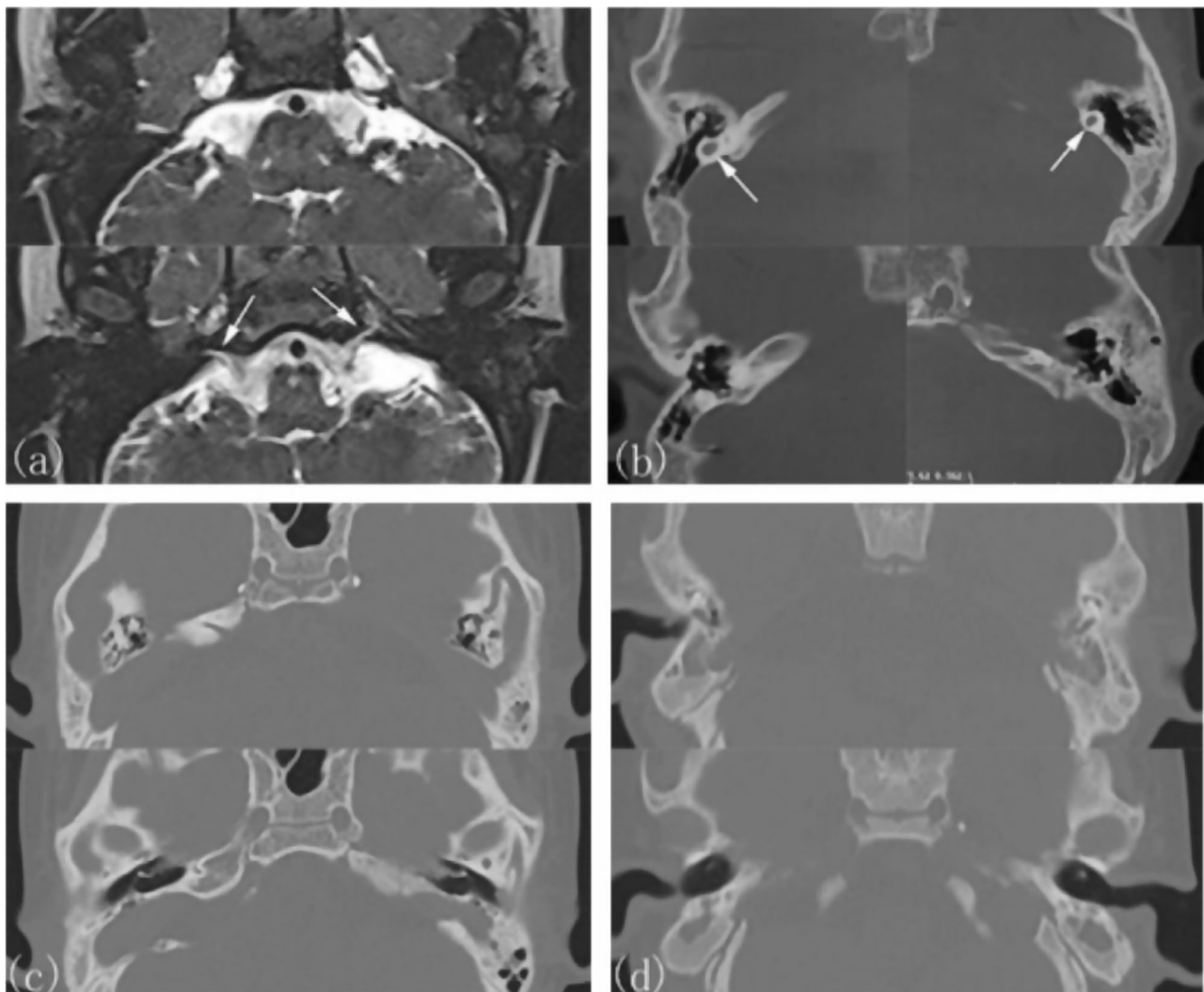


Fig. 5 MR and CT images of 4 affected individuals with complete labyrinthine aplasia, microtia, and microdontia in 3 families. **(a)** Axial 3D FIESTA images at petrous bone levels show bilateral complete labyrinthine aplasia and the tracts for facial nerves (arrows) are present (family 1). **(b)** Axial CT images show bilateral rudimentary otocyst (arrows) (family 2). **(c, d)** Axial CT images show bilateral complete labyrinthine aplasia with hypoplastic petrous bone in 2 patients (family 3)

in databases and literature. We summarized known *FGF3* variants in Table 2 [7, 12–14, 18–26]. The present study identified a novel missense variant (c.137G>C, p. Arg-46Pro, NM_005247.4) in the *FGF3* gene, results in the substitution of a highly conserved arginine by proline at amino acid 46 of the FGF3 protein. This variant lies at the start of the FGF domain (44 to 181aa) of FGF3 protein (Fig. 11), which may interrupt their interaction with the FGF ligands.

The inner ear is differentiated from the ectodermal placode adjacent to the developing hindbrain [27]. It is reported that fibroblast growth factors are involved in otic placode induction and vesicle formation in the amphibian embryo [10, 27]. *FGF3* is normally expressed in a hindbrain from otic induction through the endolymphatic duct outgrowth and also in the prospective

neurosensory domain of the otic epithelium as morphogenesis initiates [27, 28]. Multiple phenotypic features have also been identified in the inner ear associated with various *FGF3* pathogenic variants in the *FGF3* knockout models [28]. *FGF* families, including *FGF10* and *FGF8* have also been shown to be involved in an FGF signaling cascade that is required in otic induction and morphogenesis in early ear development [27, 29].

Until now, the genotype-phenotype correlation of LAMM syndrome has not been thoroughly understood. In our study, variable features were observed among patients with the same variant from different families. Our study also suggested that the specific facial features (outer ear and wide space teeth, long face) could be used as diagnostic marker for LAMM syndrome. Sequencing of the *FGF3* gene is considered as a diagnostic measure

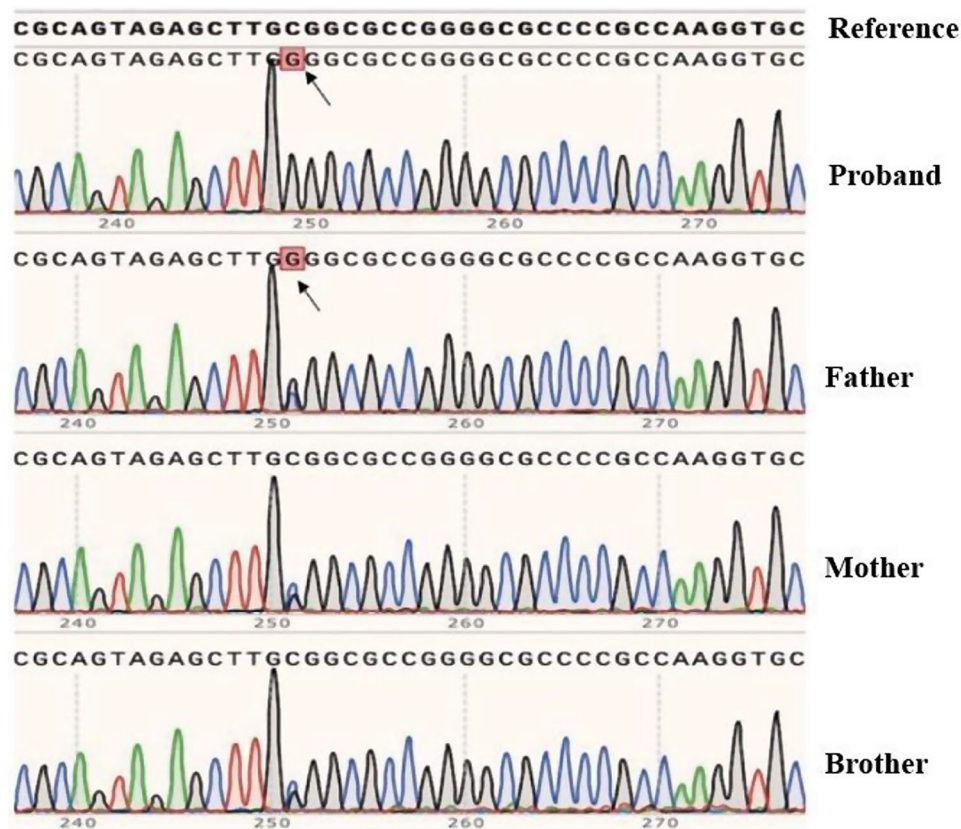


Fig. 6 The results of the Sanger sequencing of the proband and her parents and one brother in family 1. The homozygous and heterozygous mutations were found in the proband and other members of this family respectively. The arrows indicate the variant c.137G>C

which can reduce diagnostic costs when individuals present such symptoms. The variant in this study might be a founder mutation for this isolated population for which consanguineous marriage is relatively common. In future study, the haplotype of the variant could be investigated by sequencing nearby SNPs. Furthermore, the frequency of this variant should be established in order to reduce future cases for the local population. However, there were

no functional studies to investigate the function effects and the pathology of c.137G>C in *FGF3*. Instead, it is stated that additional studies are needed to show that the described variation is the responsible genetic pathology. Meanwhile, additional genotype-phenotype correlation studies will clarify the detailed phenotypic range caused by pathogenic variants in *FGF3*.

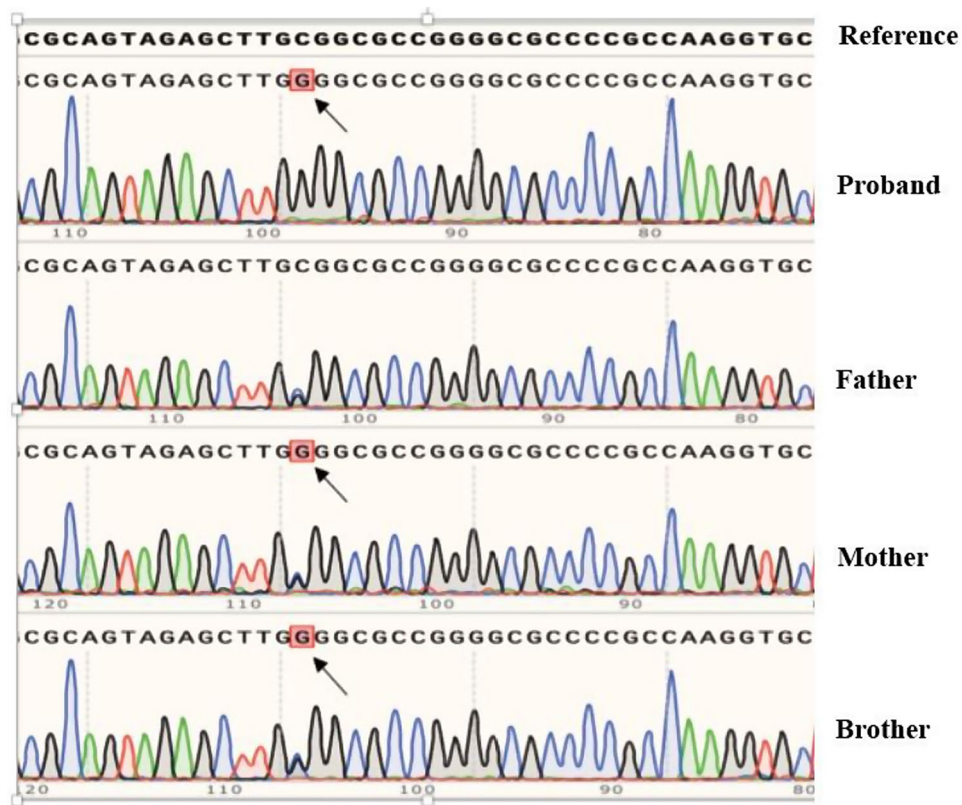


Fig. 7 The results of the Sanger sequencing of the proband and her parents and one brother in family 2. The homozygous and heterozygous mutations were found in the proband and other members of this family respectively. The arrows indicate the variant c.137G > C

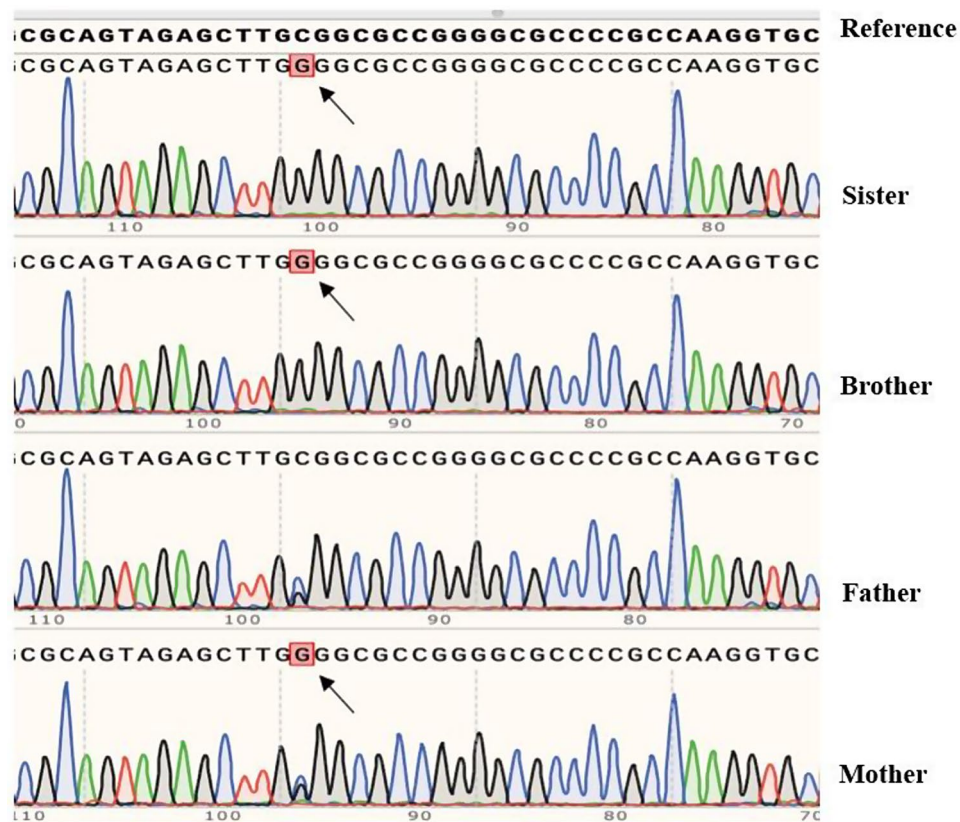


Fig. 8 The results of the Sanger sequencing of the probands and parents in family 3. The homozygous and heterozygous mutations were found in the probands and other members of this family respectively. The arrows indicate the variant c.137G>C

Table 1 Pathogenicity prediction results from multiple engines

Engine	Calibrated Prediction	Score
VEST4	Pathogenic Supporting	0.815
REVEL	Uncertain	0.588
AlphaMissense	Pathogenic Strong	0.9953
MutPred2	Pathogenic Moderate	0.739
M-CAP	Pathogenic Supporting	0.4824
Mutation assessor	Pathogenic Supporting	3.225

		46	
		↓	
<i>Homo sapiens</i>	PAAGPGARLRRDAGGRGGVYEHGGAPRR	KLYCATKYHLQLHPSGRVNG	66
<i>Pan troglodytes</i>	PAAGPGARLRRDAGGRGGVYEHGGAPRR	KLYCATKYHLQLHPSGRVNG	66
<i>Macaca mulatta</i>	PAAGPGARLRRDAGGRGGVYEHGGAPRR	KLYCATKYHLQLHPSGRVNG	66
<i>Mus musculus</i>	PTTGPGTRLRRDAGGRGGVYEHGGAPRR	KLYCATKYHLQLHPSGRVNG	66
<i>Rattus norvegicus</i>	PATGPGTRLRRDAGGRGGVYEHGGAPRR	KLYCATKYHLQLHPSGRVNG	66
<i>Canis lupus familiaris</i>	PAAGPGARLRRDAGGRGGVYEHGGAPRR	KLYCATKYHLQLHPSGRVNG	66
<i>Bos taurus</i>	PAAGPVARPRRDAGGRGGVYEHGGAPRR	KLYCATKYHLQLHPSGRVNG	66
<i>Gallus gallus</i>	PAATASPRAPRDAGGRGGVYEHGGAPRR	KLYCATKYHLQIHPGGKING	67
<i>Xenopus tropicalis</i>	RGKVC DPRRRDAGGRGGVYEHGGAPRN	KLYCATKYHLQIHLNGKING	83
<i>Danio rerio</i>	RGQACDPRRRDAGGRGGVYEHGGAPRR	KLYCATKYHLQIHPNGKIDG	84
<i>Takifugu rubripes</i>	TGAACDLRQRRDAGGRGGVYEHGGAPRR	KLYCATKYHLQIHTNGRIGG	73
<i>Gasterosteus aculeatus</i>	AGPAGHPRRRDAGGRGGVYEHGGAPRR	KLYCATKYHLQIHPNGTING	139
<i>Oryzias latipes</i>	AGQTC DPRRRDAGGRGGVYEHGGAPRR	KLYCATKYHLQIHPSGKIDG	73

Fig. 9 Arginine at position 46 of *FGF3* is conserved in a variety of organisms from fish to frogs to humans. Protein data were collected at the National Center for Biotechnology Information Web site. Protein sequences were aligned using Clustal Omega in SnapGene

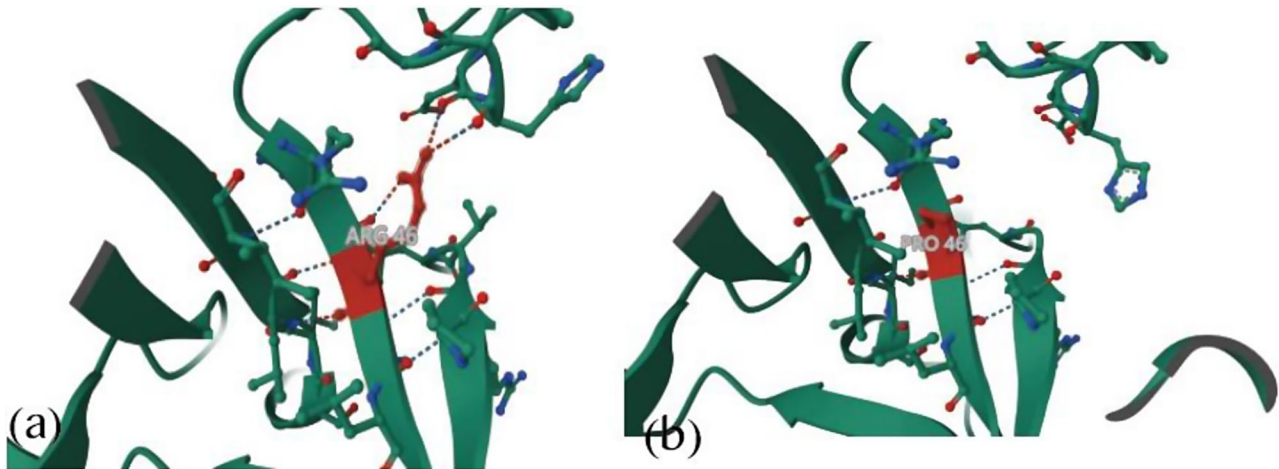


Fig. 10 3D protein structure prediction using AlphFold Protein Structure Database. (a) 3D protein structure prediction of Arginine in *FGF3*. (b) 3D protein structure prediction of Proline in *FGF3*

Table 2 Mutations found in *FGF3* gene in the literature and databases

Mutation	Reference SNP	Zygosity	Reference
c.466T>C	rs121917703	Homozygote	Tekin et al. (2007)
c.616del	rs281860305	Homozygote	Tekin et al. (2007)
c.355G>T	rs546096461	Homozygote	Tekin et al. (2007)
c.310C>T	rs121917704	Homozygote	Tekin et al. (2007); Riazuddin et al. (2011)
c.17T>C	rs121917706	Homozygote	Tekin et al. (2008)
c.254del	rs281860302	Homozygote	Tekin et al. (2008)
c.196G>T	rs121917705	Homozygote	Alsmadi et al. (2009)
c.146A>G	rs281860300	Compound Heterozygote	Sensi et al. (2011)
c.310C>T			
c.317A>G	rs281860307	Compound Heterozygote	Sensi et al. (2011)
c.457_458del			
c.394del	rs281860304	Homozygote	Riazuddin et al. (2011)
c.150C>A	rs281860301	Homozygote	Dill et al. (2011)
c.283C>T	rs281860303	Homozygote	Al Yassin et al. (2019); Ramsebner et al. (2010); Riazuddin et al. (2011)
c.284G>A	rs558206333	Compound Heterozygote	Al Yassin et al. (2019)
c.534C>G			
c.325_327delinsA	NA	Homozygote	Al Yassin et al. (2019)
c.173T>C	NA	Compound Heterozygote	Al Yassin et al. (2019)
c.283C>T			
c.196G>A	rs121917705	Homozygote	Basdemirci et al. (2019)
c.534C>G	rs782081344	Homozygote	Al Yassin et al. (2019); Lallar et al. (2021); Singh et al. (2014)
c.166C>T	rs782324453	Homozygote	Doll et al. (2020)
c.45del	rs1434810965	Homozygote	Jamshidi et al. (2023)
c.137G>C	rs887922825	Homozygote	This study
c.625C>T	rs374453035	NA	ClinVar
c.462C>G	rs782712529	NA	ClinVar
c.310dup	NA	NA	ClinVar
c.255del	rs281860302	NA	ClinVar
c.270dup	rs1444981083	NA	ClinVar

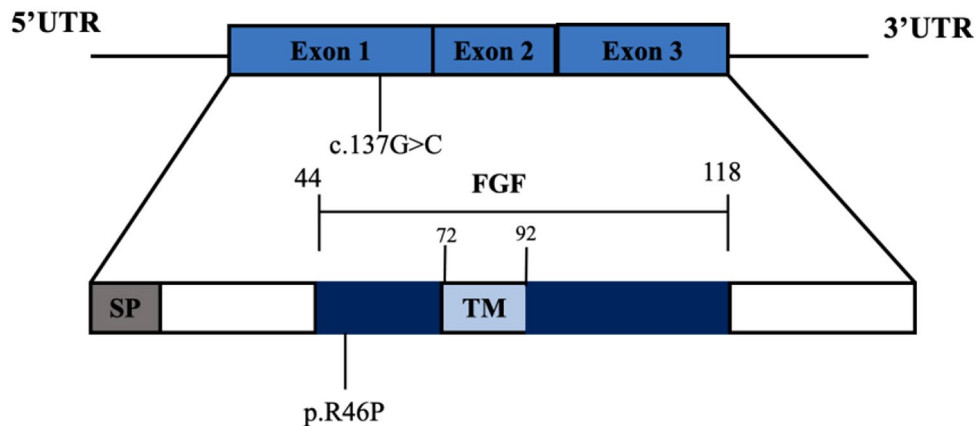


Fig. 11 The c.137G>C mutation spanning the *FGF3* gene have been associated with LAMM syndrome. The *FGF3* protein contains one highly conserved fibroblast growth factor (FGF) domain (amino acids 44–181), a predicted signal peptide (SP, amino acids 1–17), and a predicted transmembrane domain (TM, amino acids 72–92)

Conclusions

In summary, the present study identified a novel missense variant in the *FGF3* gene associated with LAMM syndrome in three unrelated Uyghur ethnic families. Novel clinical features were found in one proband from family 1. These findings expanded the variant and phenotype spectrum of LAMM syndrome and provided new insights to the diagnose and pathogenesis investigation of the disease.

Nomenclature

The DNA nomenclature throughout is concurrent with HGVS Nomenclature Version 21.0.

Web resources

AlphaMissense, <https://alphamissense.hegelab.org>.

AlphFold Protein Structure Database, <https://www.alphafold.ebi.ac.uk>.

Ensembl databases, <http://grch37.ensembl.org/index.html>.

Mendelian Clinically Applicable Pathogenicity (M-CAP), <http://bejerano.stanford.edu/mcap/>.

Mutation tasting, <https://www.mutationtaster.org>.

Mutpred2, <http://mutpred.mutdb.org/index.html>.

Online Mendelian Inheritance in Man (OMIM), <http://www.ncbi.nlm.nih.gov/Omim/>.

Rare Exome Variant Ensemble Learner'(REVEL), <https://sites.google.com/site/revelgenomics/>.

gnomAD v4.0.0 database, <https://gnomad.broadinstitute.org>.

Primer3, http://frodo.wi.mit.edu/cgi-bin/primer3/primer3_www.cgi.

Protein-protein BLAST, <http://www.ncbi.nlm.nih.gov/blast/Blast.cgi>.

HGVS Nomenclature, <https://hgvs-nomenclature.org>.

Author contributions

LG and HL designed the experiment. QD, YZ and RH carried out the experiments. QD, YZ and LG wrote the main manuscript text and prepared figures. All authors reviewed and approved the final manuscript.

Funding

This work was supported by the Natural Science Fund of Xinjiang Uygur Autonomous Region (2022D01F16), the National Natural Science Foundation of China (Nos. 82192860, 81620108005, 81500801, 81830029), the National Key R&D Program of China (Nos. 2017YFA0103900, 2016YFC0905200) and the Shanghai Municipal Health Commission (Nos. 201840277).

Data availability

The variant has been submitted to the NCBI ClinVar database whose accession number is SCV004697337. The raw sequence datasets generated during the study are not publicly available because it is possible that individual privacy could be compromised but they are available from the corresponding author Luo Guo (guoluo.gary@foxmail.com) on reasonable request.

Declarations

Ethics approval and consent to participate

All procedures performed in this study involving human participants were performed in accordance with the Declaration of Helsinki. This study was approved by the Eye, Ear, Nose and Throat Hospital affiliated with Fudan University Review Board of the Office of Research Compliance through protocol 2017044. Written informed consent was obtained from adult participants involved in the study. Written informed consent was obtained from parents/guardians of all minor participants involved in the study. This study was approved by the ethics committee of the Institutional Review Board of the Eye, Ear, Nose and Throat Hospital affiliated with Fudan University (Shanghai, China).

Consent for publication

We confirm that parents of the patients signed written informed consent for publication of their own and children's data and any accompanying images.

Competing interests

The authors declare no competing interests.

Received: 8 September 2023 / Accepted: 7 October 2024

Published online: 18 October 2024

References

- Petit C. Genes responsible for human hereditary deafness: symphony of a thousand. *Nat Genet.* 1996;14(4):385–91.

2. Morton NE. Genetic epidemiology of hearing impairment. *Ann NY Acad Sci*. 1991;630:16–31.
3. Lewis M, Robson CD, D'Arco F. Syndromic hearing loss in children. *Neuroimaging Clin N Am*. 2023;33(4):563–80.
4. Sheffield AM, Smith RJH. The epidemiology of deafness. *Cold Spring Harb Perspect Med* 2019, 9(9).
5. Petit C. From deafness genes to hearing mechanisms: harmony and counterpoint. *Trends Mol Med*. 2006;12(2):57–64.
6. Joshi VM, Navlekar SK, Kishore GR, Reddy KJ, Kumar EC. CT and MR imaging of the inner ear and brain in children with congenital sensorineural hearing loss. *Radiographics*. 2012;32(3):683–98.
7. Tekin M, Hismi BO, Fitoz S, Ozdag H, Cengiz FB, Sirmaci A, Aslan I, Inceoglu B, Yuksel-Konuk EB, Yilmaz ST, et al. Homozygous mutations in fibroblast growth factor 3 are associated with a new form of syndromic deafness characterized by inner ear agenesis, microtia, and microdontia. *Am J Hum Genet*. 2007;80(2):338–44.
8. Ordóñez J, Tekin M. Congenital Deafness with Labyrinthine Aplasia, Microtia, and Microdontia. In: *GeneReviews*(®). Edited by Adam MP, Feldman J, Mirzaa GM, Pagon RA, Wallace SE, Bean LH, Gripp KW, Amemiya A. Seattle (WA); 1993.
9. Brookes S, Smith R, Casey G, Dickson C, Peters G. Sequence organization of the human int-2 gene and its expression in teratocarcinoma cells. *Oncogene*. 1989;4(4):429–36.
10. Frenz DA, Liu W, Cvekl A, Xie Q, Wassef L, Quadro L, Niederreither K, Maconochie M, Shanske A. Retinoid signaling in inner ear development: a Goldilocks phenomenon. *Am J Med Genet A*. 2010;152A(12):2947–61.
11. Represa J, Leon Y, Miner C, Giraldez F. The int-2 proto-oncogene is responsible for induction of the inner ear. *Nature*. 1991;353(6344):561–3.
12. Tekin M, Ozturkmen Akay H, Fitoz S, Birnbaum S, Cengiz FB, Sennaroglu L, Incesulu A, Yuksel Konuk EB, Hasanefendioglu Bayrak A, Senturk S, et al. Homozygous FGF3 mutations result in congenital deafness with inner ear agenesis, microtia, and microdontia. *Clin Genet*. 2008;73(6):554–65.
13. Alsmadi O, Meyer BF, Alkuraya F, Wakil S, Alkayal F, Al-Saud H, Ramzan K, Al-Sayed M. Syndromic congenital sensorineural deafness, microtia and microdontia resulting from a novel homoallelic mutation in fibroblast growth factor 3 (FGF3). *Eur J Hum Genet*. 2009;17(1):14–21.
14. Sensi A, Ceruti S, Trevisi P, Gualandi F, Busi M, Donati I, Neri M, Ferlini A, Martini A. LAMM syndrome with middle ear dysplasia associated with compound heterozygosity for FGF3 mutations. *Am J Med Genet A*. 2011;155A(5):1096–101.
15. Du Q, Sun Q, Gu X, Wang J, Li W, Guo L, Li H. Novel homozygous variant in the PDZD7 gene in a family with nonsyndromic sensorineural hearing loss. *BMC Med Genomics*. 2022;15(1):135.
16. Li MM, Tayoun AA, DiStefano M, Pandya A, Rehm HL, Robin NH, Schaefer AM, Yoshinaga-Itano C, Practice AP, Guidelines Committee. Electronic address dan: clinical evaluation and etiologic diagnosis of hearing loss: a clinical practice resource of the American College of Medical Genetics and Genomics (ACMG). *Genet Med*. 2022;24(7):1392–406.
17. Green RC, Berg JS, Grody WW, Kalia SS, Korf BR, Martin CL, McGuire AL, Nussbaum RL, O'Daniel JM, Ormond KE, et al. ACMG recommendations for reporting of incidental findings in clinical exome and genome sequencing. *Genet Med*. 2013;15(7):565–74.
18. Riazuddin S, Ahmed ZM, Hegde RS, Khan SN, Nasir I, Shaukat U, Riazuddin S, Butman JA, Griffith AJ, Friedman TB, et al. Variable expressivity of FGF3 mutations associated with deafness and LAMM syndrome. *BMC Med Genet*. 2011;12:21.
19. Dill P, Schneider J, Weber P, Trachsel D, Tekin M, Jakobs C, Thony B, Blau N. Pyridoxal phosphate-responsive seizures in a patient with cerebral folate deficiency (CFD) and congenital deafness with labyrinthine aplasia, microtia and microdontia (LAMM). *Mol Genet Metab*. 2011;104(3):362–8.
20. Al Yassin A, D'Arco F, Morin M, Pagarkar W, Harrop-Griffiths K, Shaida A, Fernandez E, Cullup T, De-Souza B, Moreno-Pelayo MA et al. Three new mutations and mild, asymmetrical phenotype in the highly distinctive LAMM syndrome: a report of eight further cases. *Genes (Basel)* 2019, 10(7).
21. Ramsebner R, Ludwig M, Parzefall T, Lucas T, Baumgartner WD, Bodamer O, Cengiz FB, Schoefer C, Tekin M, Frei K. A FGF3 mutation associated with differential inner ear malformation, microtia, and microdontia. *Laryngoscope*. 2010;120(2):359–64.
22. Basdemirci M, Zamani AG, Sener S, Tassoker M, Cetmili H, Zamani A, Aydogdu D, Basdemirci A, Yildirim MS. LAMM syndrome: two new patients with a novel mutation in FGF3 gene and additional clinical findings. *Clin Dysmorphol*. 2019;28(2):81–5.
23. Lallar M, Arora V, Saxena R, Puri RD, Verma IC. Complete labyrinthine aplasia: a Unique sign for targeted genetic testing in hearing loss. *J Pediatr Genet*. 2021;10(1):70–3.
24. Singh A, Tekin M, Falcone M, Kapoor S. Delayed presentation of rickets in a child with labyrinthine aplasia, microtia and microdontia (LAMM) syndrome. *Indian Pediatr*. 2014;51(11):919–20.
25. Doll J, Vona B, Schnapp L, Ruschendorf F, Khan I, Khan S, Muhammad N, Alam Khan S, Nawaz H, Khan A et al. Genetic spectrum of syndromic and non-syndromic hearing loss in Pakistani families. *Genes (Basel)* 2020, 11(11).
26. Jamshidi F, Shokouhian E, Mohseni M, Kahrizi K, Najmabadi H, Babanejad M. Identification of a homozygous frameshift mutation in the FGF3 gene in a consanguineous Iranian family: first report of labyrinthine aplasia, microtia, and microdontia syndrome in Iran and literature review. *Mol Genet Genomic Med*. 2023;11(5):e2168.
27. Wright TJ, Mansour SL. Fgf3 and Fgf10 are required for mouse otic placode induction. *Development*. 2003;130(15):3379–90.
28. Hatch EP, Noyes CA, Wang X, Wright TJ, Mansour SL. Fgf3 is required for dorsal patterning and morphogenesis of the inner ear epithelium. *Development*. 2007;134(20):3615–25.
29. Ladher RK, Wright TJ, Moon AM, Mansour SL, Schoenwolf GC. FGF8 initiates inner ear induction in chick and mouse. *Genes Dev*. 2005;19(5):603–13.

Publisher's note

Springer Nature remains neutral with regard to jurisdictional claims in published maps and institutional affiliations.